Nanoscale Metal−Organic Frameworks for the Co-Delivery of Cisplatin and Pooled siRNAs to Enhance Therapeutic Efficacy in Drug-Resistant Ovarian Cancer Cells

Chunbai He, Kuangda Lu, Demin Liu, and Wenbin Lin*

Department of Chemistry, University of Chicago, 929 E 57th St, Chicago, Illinois 60637, United States

Ⓢ *Supporting Information*

ABSTRACT: Ovarian cancer is the leading cause of death among women with gynecological malignancies. Acquired resistance to chemotherapy is a major limitation for ovarian cancer treatment. We report here the first use of nanoscale metal−organic frameworks (NMOFs) for the co-delivery of cisplatin and pooled small interfering RNAs (siRNAs) to enhance therapeutic efficacy by silencing multiple drug resistance (MDR) genes and resensitizing resistant ovarian cancer cells to cisplatin treatment. UiO NMOFs with hexagonal-plate morphologies were loaded with a cisplatin prodrug and MDR gene-silencing siRNAs (Bcl-2, P-glycoprotein [P-gp], and survivin) via encapsulation and surface coordination, respectively. NMOFs protect siRNAs from nuclease degradation, enhance siRNA cellular uptake, and promote siRNA escape from endosomes to silence MDR genes in cisplatin-resistant ovarian cancer cells. Co-delivery of cisplatin and siRNAs with NMOFs led to an order of magnitude enhancement in chemotherapeutic efficacy *in vitro*, as indicated by cell viability assay, DNA laddering, and Annexin V staining. This work shows that NMOFs hold great promise in the co-delivery of multiple therapeutics for effective treatment of drug-resistant cancers.

Ovarian cancer is the deadliest gynecologic cancer with a high-mortality rate that has remained unchanged in the past four decades.[1,2] The dismal prognosis of ovarian cancer is in large part due to the acquired resistance to chemotherapy.[3] Epithelial ovarian cancer, the most common type of ovarian cancer, is initially responsive to cisplatin therapy.[4] The recurrent disease, however, is often refractory to treatment and leads to mortality.[5] New strategies to overcome drug resistance are urgently needed in order to reduce the mortality rate of ovarian cancer.

The discovery of small interfering RNA (siRNA) in 1998 has provided new avenues of combating resistant cancers.[6] Silencing genes that are involved in drug resistance using RNA interference (RNAi) can reverse cisplatin resistance in ovarian cancer.[7−10] Successful treatment of ovarian cancer cells with multidrug resistance (MDR) gene-silencing siRNAs and cisplatin requires the development of novel vehicles that can specifically and effectively deliver cisplatin to cell nuclei and siRNAs to cell cytoplasms, respectively. We report here the first use of nanoscale metal−organic frameworks (NMOFs) for the co-delivery of cisplatin and pooled siRNAs to overcome drug resistance in ovarian cancer cells.

MOFs are an emerging class of self-assembled, porous materials whose properties can be readily tuned by varying the molecular building blocks.[11−15] When scaled down to the nanoregime, NMOFs serve as efficient nanocarriers for the delivery of imaging contrast agents and chemotherapeutics.[16−21] We surmised that NMOFs represent a unique nanocarrier platform by virtue of their high porosity and controllable surface functionalities: the large pores of NMOFs can be used to load chemotherapeutics, while the metal ions on the NMOF surfaces can be used to bind siRNAs. The simultaneous and efficient delivery of cisplatin and pooled siRNAs to ovarian cancer cells can allow for enhanced anticancer efficacy by blocking multiple drug resistance pathways. In this work, a cisplatin prodrug and siRNA were sequentially loaded into UiO NMOFs by encapsulation inside the NMOFs and coordinating to metal sites on the NMOF surfaces, respectively. UiO protects siRNAs from nuclease degradation, enhances siRNA cellular uptake, and promotes siRNA escape from endosomes to silence MDR genes in cisplatin-resistant ovarian cancer cells. As a result, co-delivery of cisplatin and siRNAs with UiO led to an order of magnitude enhancement in chemotherapeutic efficacy *in vitro*.

The UiO series of MOFs based on $Zr_6(\mu_3\text{-O})_4(\mu_3\text{-OH})_4$ secondary building units (SBUs) and dicarboxylate bridging ligands first reported by Lillerud et al. are highly porous and stable in aqueous environment due to the high connectivity of the SBUs and the strong interaction between zirconium and oxygen.[22] UiO NMOFs thus represent potential nanocarriers for anticancer drugs. In this work, the UiO NMOF with amino-triphenyldicarboxylic acid (amino-TPDC) bridging ligand was synthesized by heating a *N,N*-dimethylformamide (DMF) solution of $ZrCl_4$ and amino-TPDC at 80 °C for 5 days (Figure 1a and Scheme S1).[23] The as-synthesized NMOF adopted a distorted UiO structure as manifested by powder X-ray diffraction (PXRD), which was likely responsible for its hexagonal plate-like morphology as shown in transmission electron microscopy (TEM) images (Figure 1b−g). TEM micrographs gave the diameter of the plate at ∼100 nm and the thickness at ∼30 nm (Figure 1b−d). High-resolution TEM images showed that the distances between the lattice fringes are 1.83 nm (Figures 1f and S6 and 10), corresponding to the
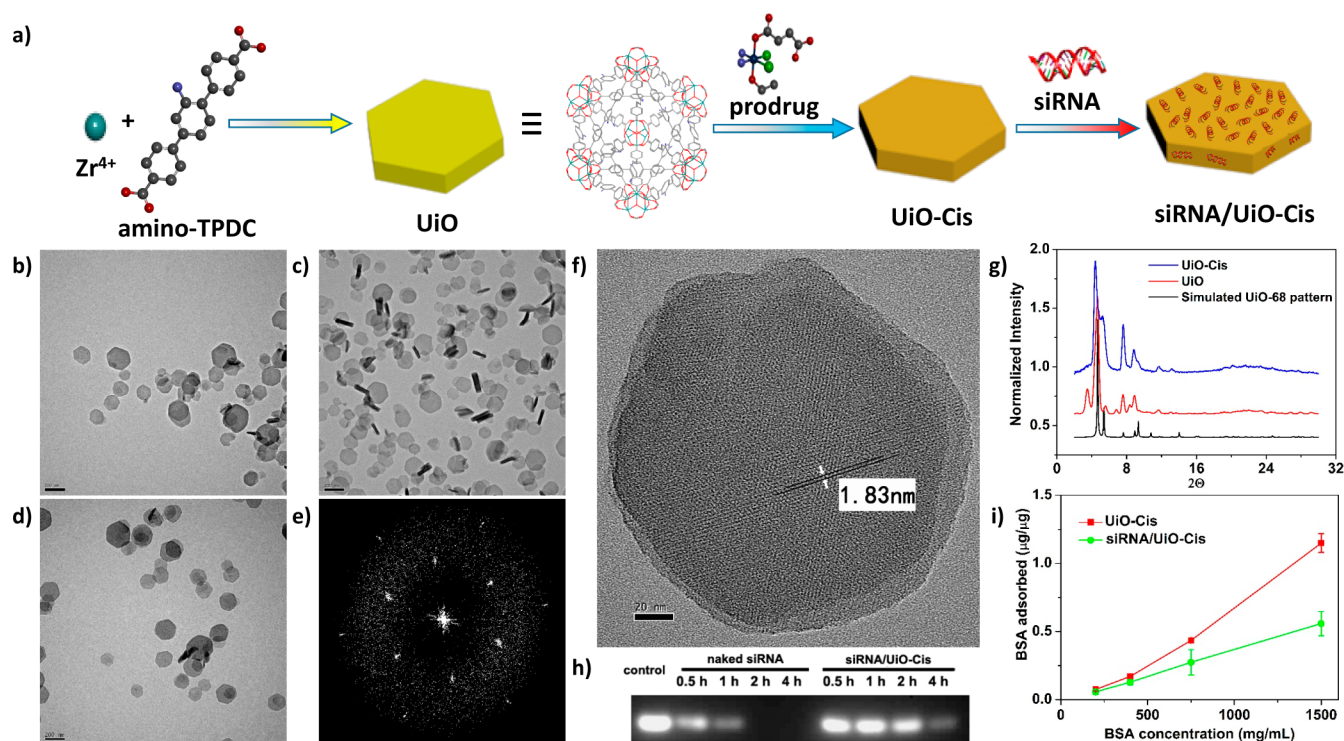
Figure 1. Preparation and characterization of siRNA/UiO-Cis. (a) Schematic presentation of siRNA/UiO-Cis synthesis and drug loading. TEM images of UiO (b), UiO-Cis (c), and siRNA/UiO-Cis (d). Bars: 200 nm. (e) Electron diffraction pattern of UiO by FFT. (f) High-resolution TEM image of UiO. Bar: 20 nm. (g) PXRD patterns of UiO-68 (black), UiO (red), and UiO-Cis (blue). (h) Serum stability of pooled siRNAs in siRNA/UiO-Cis as evaluated by electrophoresis. (i) BSA binding to UiO-Cis with and without siRNA loading. The results were expressed as the amount of BSA (μg) adsorbed to per μg of UiO-Cis.

predicted $d(111)$ value of 1.85 nm. The fast Fourier transform pattern (FFT) proved a 3-fold symmetry along the observation direction (Figure 1e). The cisplatin prodrug, *cis, cis, trans*-$[Pt(NH_3)_2Cl_2(OEt)(OCOCH_2CH_2COOH)]$,[24] was loaded into the pores of UiO via encapsulation to form UiO-Cis (Figure 1a and Scheme S2). NMR spectroscopy supported the noncovalent encapsulation of cisplatin prodrug (Figures S11−13), whereas PXRD indicated that UiO-Cis is isostructural to UiO-68 (Figure 1g). The cisplatin prodrug loading in UiO-Cis was determined to be 12.3 ± 1.2 wt % by inductively coupled plasma mass spectrometry.

Drug resistance often involves multiple and dynamically acquired MDR mechanisms. Among them, P-gp is overexpressed in the malignant tissues and is responsible for decreased drug accumulation in cells.[8] Bcl-2 is responsible for the activation of cellular antiapoptotic defense.[25,26] Survivin has a functional role in both cell division and apoptosis control and is often found to be upregulated in cancers.[27] Simultaneously blocking these MDR-relevant molecular signaling pathways can provide an effective approach for overcoming drug resistance in cancer cells. siRNA was loaded onto UiO-Cis by simply mixing UiO-Cis and siRNA in water at a cisplatin:siRNA mass ratio of 4.5:1 to form siRNA/UiO-Cis (Figure 1a). siRNA is believed to bind to NMOF surface via multiple coordination bonds between phosphate residues on the siRNA backbone and vacant Zr sites on the NMOF surface. The siRNA loading did not change the morphology of NMOFs as shown by TEM (Figure 1d). Dynamic light scattering (DLS) measurements gave average diameters of 98 ± 11 nm (PDI = 0.070), 103 ± 17 nm (PDI = 0.124), and 128 ± 3 nm (PDI = 0.116) for UiO, UiO-Cis, and siRNA/UiO-Cis, respectively (Figures S8, S10,

and S15). The increase in the DLS diameter for siRNA/UiO-Cis is consistent with the presence of siRNA on the UiO surface. The siRNA binding capabilities of NMOFs were confirmed by gel electrophoresis, which showed that NMOFs could efficiently "capture" siRNA on the surface as evidenced by the complete retardation of siRNA band migration for siRNA/UiO-Cis (Figure S16). The siRNA loading efficiency (LE) was also quantitatively examined by fluorimetry. Fluorescently labeled siRNA (TAMRA-siRNA) was used to form siRNA/UiO-Cis, and the LE was determined to be as high as 81.6 ± 0.6%. As a result of steric hindrance on surfaces, NMOFs protected siRNA from RNase degradation: a siRNA band was clearly visible upon incubating siRNA/UiO-Cis in serum for up to 4 h, while the naked siRNA was completely degraded under the same condition (Figure 1h). Interestingly, siRNA "coating" on the NMOF surface significantly retarded protein adsorption, suggesting possible stabilization of NMOFs via siRNA binding (Figure 1i).

High siRNA uptake levels and successful endosomal escape are two prerequisites for efficient siRNA-mediated gene silencing.[28−30] Compared to the naked siRNA solution, cellular uptake of siRNA/UiO-Cis was significantly enhanced (Figure 2a), indicating that the NMOF facilitates the siRNA internalization via endocytosis pathways. The siRNA uptake was also directly observed by confocal laser scanning microscopy (CLSM). As illustrated in Figures 2b and S17, large amounts of siRNA (red fluorescence) were located in the cytoplasms of SKOV-3 cells. In addition, zirconium phosphate has extremely low solubility ($K_{sp} = 10^{-134}$), which demonstrates a high affinity of Zr(IV) to phosphate ions. As illustrated in Figure 2c, phosphate buffer saline (PBS) containing relatively high
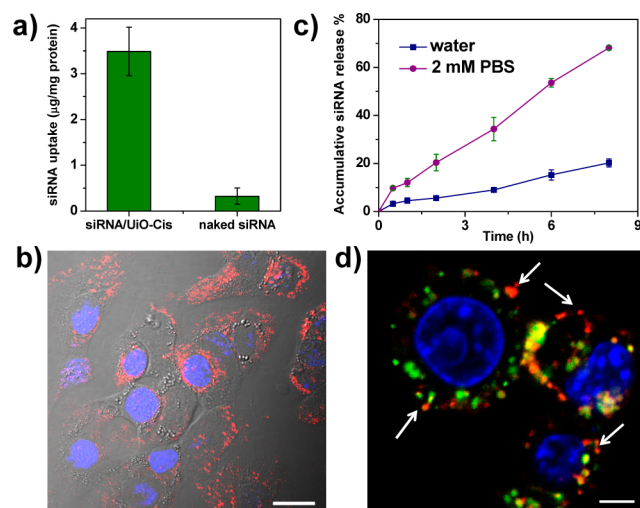
Figure 2. Cellular uptake and endosomal escape of siRNA/UiO-Cis in SKOV-3 cells. (a) siRNA/UiO-Cis significantly increase (by >11-fold) the siRNA uptake amount compared to naked siRNA ($n = 3$). (b) CLSM image showing the internalization of siRNA (TAMRA-labeled) into the cytoplasm. Nuclei were stained with DAPI. Bar represents 20 μm. (c) siRNA release from NMOFs was dramatically promoted in 2 mM PBS compared to water. (d) siRNA (TAMRA-labeled, red) successfully escaped from endosomes as evidenced by the separation of green and red fluorescence (white arrows). Endosome/lysosome and nuclei were stained with Lysotracker Green and DAPI, respectively. Bar represents 5 μm.

phosphate group concentration (2 mM) significantly promoted siRNA release compared to water. It is reasonable to expect that siRNA could dissociate from UiO-Cis and that UiO-Cis could decompose after internalization and entrapment in endosomes due to the presence of much higher concentrations of endogenous phosphate ions in endosomes than in

extracellular environments (Figure S12). The dissociated Zr ions can bind to the negatively charged and phosphate-group-enriched endosome membrane to disrupt the endosome structure and facilitate the release of entrapped siRNAs. This hypothesis was supported by CLSM studies and time-dependent endosome/siRNA colocalization studies (Figure S19 and 20). After a 2 h incubation, siRNA in the siRNA/UiO-Cis was able to escape from the endo/lysosome entrapment, as demonstrated by the separation of red (siRNA) and green (Lysotracker Green stained lysosome) fluorescence in the cytoplasm (Figures 2d and S18).

We further evaluated the transfection efficiency mediated by siRNA/UiO-Cis in SKOV-3 cells. As shown in Figure 3a, siRNA/UiO-Cis evoked potent gene silencing in SKOV-3 cells at 0.4 μg/mL (30 nM) of siRNA as determined by ELISA. Interestingly, by using one-third of the siRNA dose for the pooled siRNAs/UiO-Cis compared to single siRNA/UiO-Cis, equivalent gene silencing efficiencies were achieved, suggesting the synergistic silencing effects of pooled siRNAs. In comparison, none of the free siRNA solution, UiO-Cis, and UiO was able to down regulate the gene expression.

To examine whether the efficient and simultaneous knockdown of three MDR-relevant genes including survivin, Bcl-2, and P-gp could effectively reverse the cisplatin resistance in ovarian cancer cells, the cytotoxicity of free cisplatin, UiO-Cis, and siRNA/UiO-Cis was assessed by 3-(4,5-dimethylthiazol-2-yl)-5-(3-carboxymethoxyphenyl)-2-(4-sulfophenyl)-2H-tetrazolium (MTS) assay (Figure 3b) and by flow cytometry (Figure S26). The cisplatin IC_{50} values of free cisplatin, UiO-Cis, pooled siRNAs/UiO-Cis, free cisplatin plus free pooled siRNAs, and free cisplatin plus pooled siRNAs/UiO were calculated to be 53.9 ± 4.7, 53.2 ± 4.4, 4.7 ± 1.8, 45.1 ± 7.0, and 6.6 ± 0.3 μM, respectively. No cytotoxicity (cell viability of $96.2 \pm 3.4\%$) was observed in SKOV-3 cells when treated with
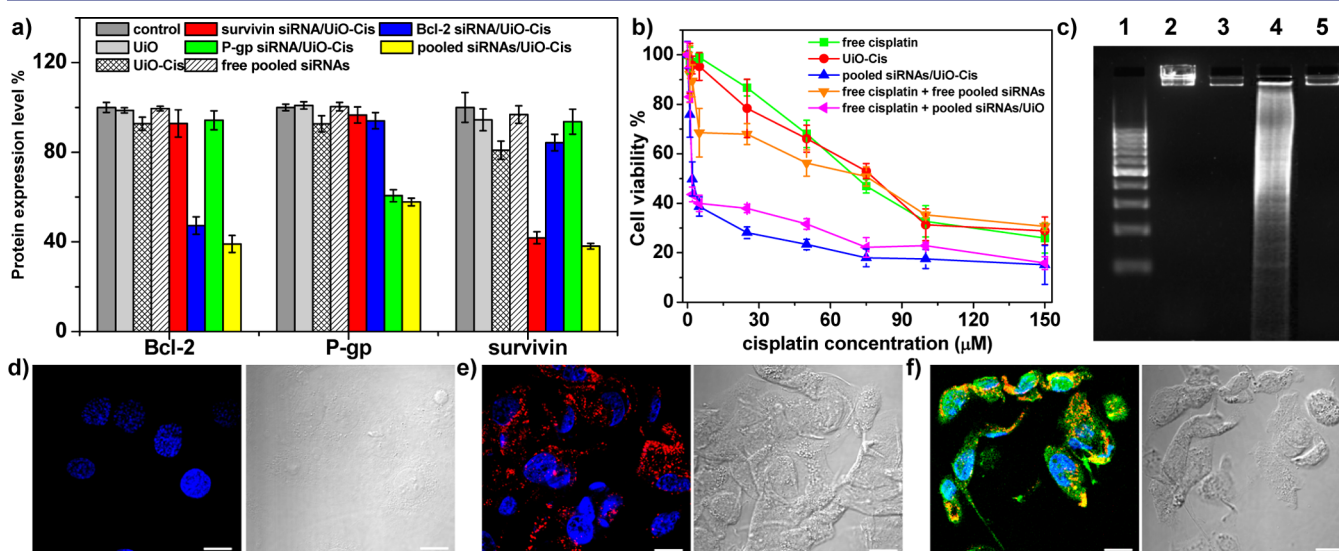

Figure 3. *In vitro* gene silencing efficiency and anticancer efficacy. (a) siRNA/UiO-Cis-mediated efficient gene silencing in SKOV-3 cells at a 30 nM siRNA dose. Silencing efficiency was expressed as percentage values of control group treated with PBS. (b) SKOV-3 cells were incubated with free cisplatin, UiO-Cis, pooled siRNAs/UiO-Cis, free cisplatin plus free pooled siRNAs, and free cisplatin plus pooled siRNAs/UiO at different concentrations for 72 h, and then the cytotoxicity was determined by MTS assay. (c) Analysis of DNA ladder on 2% (w/v) agarose gel at 35 V for 5 h after DNA extraction from SKOV-3 cells treated with siRNA/UiO-Cis at an equivalent cisplatin concentration of 10 μM. Lanes 1−5: DNA marker, control, UiO-Cis, siRNA/UiO-Cis, and free cisplatin. (d−f) CLSM images showing cell apoptosis and siRNA (TAMRA-labeled, red) internalization in SKOV-3 cells after incubation with UiO-Cis (d), siRNA/UiO (e), and siRNA/UiO-Cis (f) for 24 h. The apoptotic cells were stained with Alexa Fluor 488 Annexin V conjugate, and the nuclei were stained with DAPI. Bar represented 10 μm.

siRNA/UiO at 12 times higher siRNA dose. By co-delivering pooled siRNAs and cisplatin utilizing NMOFs, the IC_{50} value dramatically decreased (by more than 11-fold) compared to free cisplatin and UiO-Cis. In control experiments, pooled siRNAs/UiO-Cis and UiO-Cis exhibited a similar level of cytotoxicity in cisplatin-sensitive cancer cell lines including A2780, PC-3, MCF-7, and H460 cells but significantly lower IC_{50} values in cisplatin-resistant A2780/CDDP cells (4.2 ± 0.6 vs 21.4 ± 1.4 μM for pooled siRNAs/UiO-cis and UiO-Cis, respectively; Figure S21−24, Table S1). This result suggested that the cisplatin-resistant ovarian cancer cells could be resensitized after being transfected with siRNA/UiO-Cis, and the synergistic effects of siRNA and cisplatin significantly enhanced the *in vitro* chemotherapeutic efficacy. At 50 times higher UiO dose, cell viability was determined to be 98.1 ± 5.4%, indicating a lack of toxicity for UiO. We carried out DNA ladder and Annexin V conjugate staining assays in order to demonstrate that the enhanced cytotoxicity of siRNA/UiO-Cis was caused by cell apoptosis rather than necrosis. As indicated in Figure 3c, no DNA fragmentation was detectable in the control, UiO-Cis, and free cisplatin groups. Cells treated with siRNA/UiO-Cis displayed characteristic DNA fragmentation or laddering, demonstrating that the cytotoxicity induced by siRNA/UiO-Cis was associated with apoptosis. Annexin V conjugate staining provided further evidence to the apoptosis induced by siRNA/UiO-Cis (Figures 3d and S25). siRNA (red fluorescence) loaded in the NMOFs was efficiently internalized into the cytoplasm after a 24 h incubation to trigger MDR-relevant gene silencing. Annexin V conjugate (green fluorescence) was clearly visible in cells treated with siRNA/UiO-Cis but not in cells treated with siRNA/UiO (pooled siRNAs alone) or UiO-Cis (cisplatin alone). This result indicates that co-delivery of cisplatin and pooled siRNAs would induce cell apoptosis in cisplatin-resistant cells by combining the synergistic effects of down-regulating the expressions of MDR-relevant genes and chemotherapeutics. Importantly, UiO and pooled siRNAs/UiO-Cis evoked no immunogenic response in Raw 264.7 macrophage and SKOV-3 cells (Figure S27).

In summary, we have shown that UiO NMOFs with high porosity and surface binding sites represent a unique nanocarrier platform for the co-delivery of chemotherapeutic agents and pooled MDR gene silencing siRNAs to drug-resistant ovarian cancer cells. Cisplatin prodrug was efficiently loaded into UiO by encapsulation, whereas siRNA was loaded by coordinating to metal sites on the NMOF surfaces. The UiO protects siRNAs from nuclease degradation, enhances siRNA cellular uptake, and promotes siRNA escape from endosomes to silence MDR genes, leading to an order-of-magnitude enhancement in chemotherapeutic efficacy of cispltain. The simplicity of the present approach makes it amenable to co-delivery of chemotherapeutics and other nucleic acid drugs such as siRNA, microRNA, and plasmid DNA by NMOFs. We believe that this unique NMOF platform holds great promise in the treatment of difficult to cure cancers by co-delivering therapeutic cargoes of disparate characteristics and functions.

ASSOCIATED CONTENT

Ⓢ Supporting Information

Experimental details and characterization data. This material is available free of charge via the Internet at http://pubs.acs.org.

AUTHOR INFORMATION

Corresponding Author

wenbinlin@uchicago.edu

Notes

The authors declare no competing financial interest.

ACKNOWLEDGMENTS

REFERENCES

(1) Coleman, R. L.; Monk, B. J.; Sood, A. K.; Herzog, T. J. *Nat. Rev. Clin. Oncol.* **2013**, *10*, 211.

(2) Vaughan, S.; Coward, J. I.; Bast, R. C.; Berchuck, A.; Berek, J. S.; Brenton, J. D.; et al. *Nat. Rev. Cancer* **2011**, *11*, 719.

(3) Roberts, D.; Schick, J.; Conway, S.; Biade, S.; Laub, P. B.; Stevenson, J. P.; Hamilton, T. C.; O'Dwyer, P. J.; Johnson, S. W. *Br. J. Cancer* **2005**, *92*, 1149.

(4) Kelland, L. *Nat. Rev. Cancer* **2007**, *7*, 573.

(5) Lowery, W. J.; Lowery, A. W.; Barnett, J. C.; Lopez-Acevedo, M.; Lee, P. S.; Secord, A. A.; Havrilesky, L. *Gynecol. Oncol.* **2013**, *130*, 426.

(6) Fire, A.; Xu, S. Q.; Montgomery, M. K.; Kostas, S. A.; Driver, S. E.; Mello, C. C. *Nature* **1998**, *391*, 806.

(7) Yellepeddi, V. K.; Vangara, K. K.; Kumar, A.; Palakurthi, S. *Anticancer Res.* **2012**, *32*, 3651.

(8) Xiong, X. B.; Lavasanifar, A. *ACS Nano* **2011**, *5*, 5202.

(9) Meng, H.; Liong, M.; Xia, T.; Li, Z.; Ji, Z.; Zink, J. I.; Nel, A. E. *ACS Nano* **2010**, *4*, 4539.

(10) Shahzad, M. M. K.; Lopez-Berestein, G.; Sood, A. K. *Drug Resist. Update* **2009**, *12*, 148.

(11) Li, H.; Eddaoudi, M.; O'Keeffe, M.; Yaghi, O. M. *Nature* **1999**, *402*, 276.

(12) Dinca, M.; Long, J. R. *Angew. Chem., Int. Ed.* **2008**, *47*, 6766.

(13) Rosi, N. L.; Kim, J.; Eddaoudi, M.; Chen, B. L.; O'Keeffe, M.; Yaghi, O. M. *J. Am. Chem. Soc.* **2005**, *127*, 1504.

(14) Lee, J.; Farha, O. K.; Roberts, J.; Scheidt, K. A.; Nguyen, S. T.; Hupp, J. T. *Chem. Soc. Rev.* **2009**, *38*, 1450.

(15) Wang, Z. Q.; Cohen, S. M. *Chem. Soc. Rev.* **2009**, *38*, 1315.

(16) Rieter, W. J.; Taylor, K. M. L.; An, H.; Lin, W.; Lin, W. *J. Am. Chem. Soc.* **2006**, *128*, 9024.

(17) Rieter, W. J.; Pott, K. M.; Taylor, K. M. L.; Lin, W. *J. Am. Chem. Soc.* **2008**, *130*, 11584.

(18) Dekrafft, K. E.; Xie, Z.; Cao, G.; Tran, S.; Ma, L.; Zhou, O. Z.; Lin, W. *Angew. Chem., Int. Ed.* **2009**, *48*, 9901.

(19) Taylor-Pashow, K. M. L.; Della Rocca, J.; Xie, Z.; Tran, S.; Lin, W. *J. Am. Chem. Soc.* **2009**, *131*, 14261.

(20) Horcajada, P.; Chalati, T.; Serre, C.; Gillet, B.; Sebrie, C.; Baati, T.; et al. *Nat. Mater.* **2010**, *9*, 172.

(21) Liu, D.; Huxford, R. C.; Lin, W. *Angew. Chem., Int. Ed.* **2011**, *50*, 3696.

(22) Cavka, J. H.; Jakobsen, S.; Olsbye, U.; Guillou, N.; Lamberti, C.; Bordiga, S.; Lillerud, K. P. *J. Am. Chem. Soc.* **2008**, *130*, 13850.

(23) Schaate, A.; Roy, P.; Godt, A.; Lippke, J.; Waltz, F.; Wiebcke, M.; Behrens, P. *Chem.—Eur. J.* **2011**, *17*, 6643.

(24) Zou, S.; Cao, N.; Cheng, D.; Zheng, R.; Wang, J.; Zhu, K.; Shuai, X. *Int. J. Nanomed.* **2012**, *7*, 3823.

(25) Feazell, R. P.; Nakayama-Ratchford, N.; Dai, H.; Lippard, S. J. *J. Am. Chem. Soc.* **2007**, *129*, 8438.

(26) Chen, A. M.; Zhang, M.; Wei, D.; Stueber, D.; Taratula, O.; Minko, T.; He, H. *Small* **2009**, *5*, 2673.

(27) Cho, Y. S.; Lee, G. Y.; Sajja, H. K.; Qian, W. P.; Cao, Z. H.; He, W. L.; Karna, P.; Chen, X. Y.; Mao, H.; Wang, Y. A.; Yang, L. *Small* **2013**, *9*, 1964.

(28) Foged, C. *Curr. Top. Med. Chem.* **2012**, *12*, 97.

(29) Zhang, K.; Hao, L. L.; Hurst, S. J.; Mirkin, C. A. *J. Am. Chem. Soc.* **2012**, *134*, 16488.

(30) Cutler, J. I.; Auyeung, E.; Mirkin, C. A. *J. Am. Chem. Soc.* **2012**, *134*, 1376.